RECEIVED BY OSTI DEC 06 1985

LA-UR-85-3785

Los Alamos National Laboratory is operated by the University of California for the United States Department of Energy under contract W-7405-ENG-36

TITLE ION BEAM CHARACTERIZATION OF MULTI-LAYER DIELECTRIC REFLECTORS

LA-UR--85-3785

DE86 003689

AUTHOR(S) Jerome G. Beery, E-11
Mark G. Hollander, E-11
Carl J. Maggiore, E-11
Antonio Redondo, E-11
Thomas N. Taylor, CHM-2

SUBMITTED TO Proceedings on Optical Materials for High-Power Lasers, Boulder, CO, October 28-30, 1985

DISCLAIMER

MASTER

Los Alamos Los Alamos National Laboratory
Los Alamos, New Mexico 87545

Ion Beam Characterization of Multi-Layer Dielectric Reflectors

J. G. Beery, M. G. Hollander, C. J. Maggiore,
A. Redondo, R. T. Westervelt, and T. N. Taylor

Los Alamos National Laboratory
Los Alamos, NM 87545

Energetic ion beams were used to characterize multilayer dielectric reflectors. Alpha-particle beams with beam spot sizes between 10 microns and a few millimeters were scattered from reflectors consisting of 32-layer SiO_2/HfO_2 and 38-layer MgF_2/ThF_4. The RBS spectra reveal the nature of the laser damage processes by providing information on diffusion, mixing, and loss of material in the coatings. The particle-induced x-ray emission (PIXE) technique gave complimentary results on low-concentration impurities in the coatings.

Key Words: dielectric reflectors, nuclear microprobe, particle-induced x-ray emission, Rutherford backscattering.

1 Introduction

Considerable work in the damage mechanisms of multilayer dielectric reflectors has previously been reported, using a variety of experimental techniques. The fundamental damage mechanisms are not completely understood because of the complexity of the systems. We have carried out Rutherford backscattering [1] (RBS) and particle-induced x-ray emission [2] (PIXE) experiments using energetic ion beams to characterize high-reflection coatings on laser mirrors before and after damage. These experiments are particularly suitable for measuring the composition as a function of depth, the presence of low concentration impurities, and changes in the structure of the films as a result of the damage processes. The measurements have been made on undamaged coatings with spot sizes of a few square millimeters. Localized structure in the region of individual damage pits has been studied using a nuclear microprobe [3,4], which produces spot sizes as small as ten microns in diameter. The RBS spectra obtained provide information about damage profiles, mixing, diffusion, and loss of material in the coatings. The PIXE technique has been used to measure low concentration levels of impurities in the films.

2 Experimental Method

Rutherford backscattering is a well-established quantitative technique for interface and thin film analysis. It is an analytical technique based on known kinematics and energy loss that can determine the composition and structure in materials to a depth of a few microns.

Figure 1 is a schematic drawing of the general geometry of a backscattering experiment. A beam of light ions from a Van de Graaff accelerator strikes a target, and the scattered particles are detected with a surface barrier detector at a fixed angle. Figure 1a shows a thin film of a heavy element on top of a lighter substrate. The observed energy of the backscattered particles is determined by the kinematics of the elastic scattering and the depth of the scattering event below the surface. Figure 1b shows a typical RBS spectrum. The highest energy, KE_{in}, corresponds to elastic scattering at the surface of the film. The energy E_f is due to elastic scattering from the film at the film substrate interface and the energy loss of the particles traversing the film. The width of the peak, ΔE, is related to the areal density (atoms/cm^2) of the film. The relative masses of the incident and target particles and the scattering geometry determine the kinematic factor, K. The backscattering energy increases with the mass of the target atoms. Thus, RBS is particularly well suited for measuring the distribution of heavy elements in a lighter matrix.

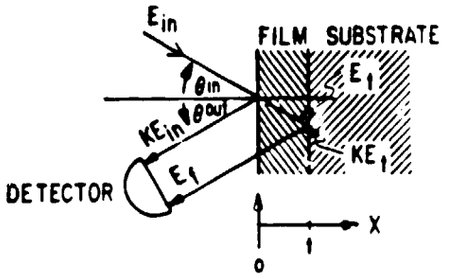

Figure 1a. General backscattering geometry for Rutherford backscattering measurement.

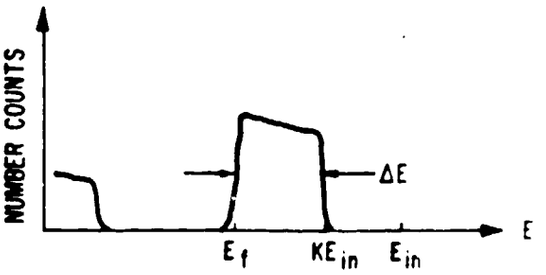

Figure 1b. RBS spectrum obtained from a heavy thin film on a light substrate.

The RBS experiments reported here were carried out with 2.3 and 2.5 MeV α-particles with $\theta_{in} = 0$ and $\theta_{out} = 20$ degrees. We studied 32-layer SiO_2/HfO_2 and 38-layer MgF_2/ThF_4 coatings on fused silica. Since the kinematic factor for the lighter elements, Si, O, Mg and F, is much less than that for the Hf or Th, the high energy part of the spectrum characterizes the depth distribution of the heavy elements in the film.

The technique favors high Z elements because the Rutherford backscattering cross section is proportional to Z^2. If the elemental masses are too close, the kinematic constraints limit the mass resolution and result in overlapping spectra for compound samples. Consequently, the analysis of Al_2O_3/SiO_2 coatings is somewhat more difficult. These factors, together with finite detector resolution, limit our depth sensitivity at the surface to approximately 50 angstroms. Energy straggling degrades depth resolution below the surface.

When an energetic ion looses energy in the sample, it induces x-ray emission characteristic of the atoms in the target. Energy analysis of these characteristic lines permits elemental identification at low concentration levels. The PIXE technique is generally applicable to atoms with Z > 10. The sensitivity depends on the matrix and the atomic number and is usually in the range of 10 ppm. For the work reported here, the incident beam was 2.0 MeV protons.

These techniques can be applied to the study of localized damage by focusing the incident ion beam into small spatial dimensions. We have studied individual damage pits on multilayer dielectric reflectors using these focused ion beams with both the RBS and PIXE techniques. A nuclear microprobe with spot sizes of a few microns in diameter was used.

We studied SiO_2/HfO_2 and MgF_2/ThF_4 multilayer coatings on fused silica substrates. The structure of these films is given in Table 1. Table 2 describes the dimensions of the beam spots and the resulting current densities. For the two larger spot sizes, the RBS and PIXE techniques are non-destructive. For the smallest spot size of ten microns, the current density is high enough to create color centers.

Table 1. Structure of multilayer dielectric reflectors.

HR351 166 SPP	351 nm
$(H\ L)^{10}$ H (L H 4/9 H 0.70 L)	
H HfO_2	
L SiO_2	
HR248 213 OCLI	248 nm
$(HL)^{19}H$	
H ThF_4	
L MgF_2	

Table 2. α-particle beam parameters.

SPOT SIZE	CURRENT (nA)	CURRENT DENSITY A/cm²
5 mm x 5 mm	20	8×10^{-4}
r = 100 μ	5	6×10^{-1}
r = 10 μ	2	3×10^{1}

3. Results

Figure 2 shows the experimental RBS energy spectrum from the SiO_2/HfO_2 coating. One can clearly see 16 separate hafnium peaks. Also evident is the change in layer thickness for the topmost five layers of HfO_2. The silicon contribution overlaps the lower energy portion of the hafnium peaks extending up to 1.4 MeV, but it does not significantly alter the spectrum due to its lower scattering cross section. The low energy cutoff at 200 keV is due to the discriminator setting in the electronics.

Similar data were also taken on an undamaged MgF_2/ThF_4 coating. These results are shown in Figure 3. The first 15 layers of this spectrum have been simulated using the model parameters listed in Table 3. The simulation was performed using computer programs based on first principles for the scattering and parameterized energy loss equations. The input consists of average stoichiometric ratios for the individual elements in each layer. The program uses them to calculate the corresponding spectra which are then compared with experiment. The best fit was achieved with a decreasing ratio of thorium to fluorine as one moves toward the substrate (e.g., 1 to 4 for the top layer and 1 to 5 for the eighth layer). In addition, the thorium that is missing from a given ThF_4 layer appears uniformly distributed in the adjacent MgF_2 layer. This can be interpreted as evidence for interlayer mixing during the fabrication process. The thorium fluoride layers are uniform to within 5%. The magnesium fluoride layers appear to be fairly uniform; however, the simulation is not very sensitive to the low mass layers.

Figure 4 is a Nomarski micrograph of a laser damage spot in the silica/hafnia coating. The large oval feature at the center is the visibly damaged region that penetrates to the substrate. The striations to the left and right were made visible during or after the damage process. A relatively clear area

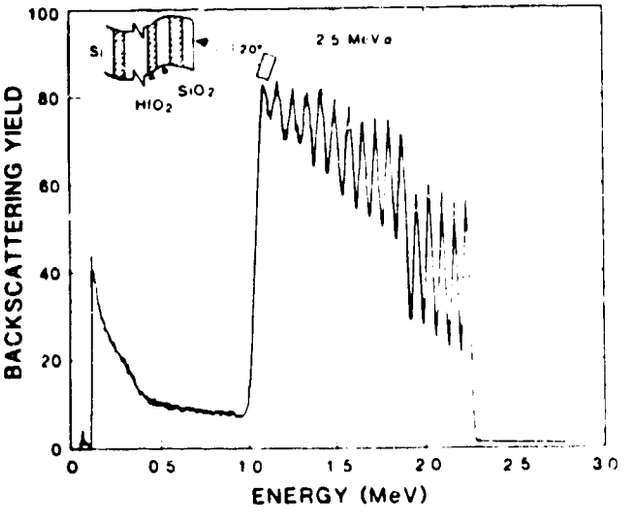

Figure 2. RBS energy spectrum for undamaged region of SiO_2/HfO_2 reflector.

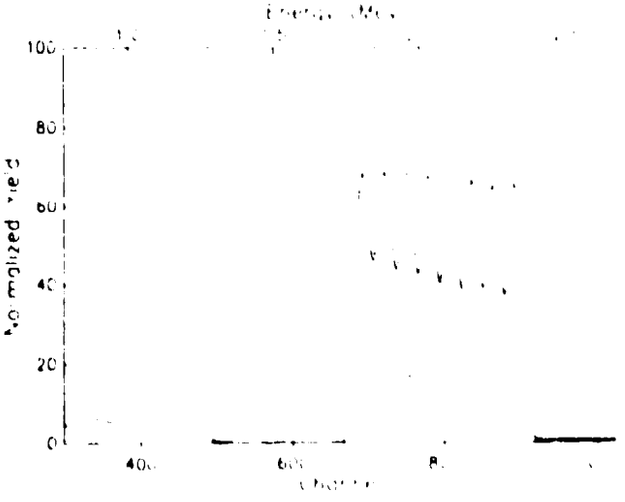

Figure 3. RBS energy spectrum for undamaged region of MgF_2/ThF_4 reflector (points). Simulated spectrum for fifteen layers nearest surface (solid line).

Table 3. Simulated structure for fifteen layers of MgF_2/ThF_4. Layer 1 is at the surface.

Layer No.	Thickness (10^{15} atoms/cm^2)	Atomic Concentration (%) Th	F	Mg
1	405	20.0	80.0	
2	430		66.7	33.3
3	410	18.9	81.1	
4	430	1.0	66.0	33.0
5	410	18.5	81.5	
6	430	1.0	66.0	33.0
7	410	18.2	81.8	
8	428	1.6	65.6	32.8
9	405	17.5	82.5	
10	428	2.6	64.9	32.5
11	387	17.4	82.6	
12	428	3.2	64.5	32.3
13	405	16.1	83.9	
14	428	4.2	63.9	31.9
15	410	16.1	83.9	

immediately adjacent to the damage pit suggests that these striations were annealed by thermal processes. To study in detail the damage at a single pit, we focused the ion beam to a spot 10 microns in diameter using the nuclear microprobe. The line of small spots across the lower part of the oval feature is due the microprobe ion beam. We believe that the radiation damage from the ion beam created color centers.

Figure 4. Nomarski micrograph of laser damaged spot and surrounding region

For the line scan across the laser damage area we obtained RBS spectra, one spectrum at each spot. Figure 5 is a composite of five spectra taken at various positions near or on the laser-damaged area of figure 4. The widest spectrum corresponds to the microprobe analysis at the edge of the damaged region and is similar to that of figure 2 except that the statistics are poorer. In addition, there is a small surface peak corresponding to hafnium that has been ejected from the pit and is on top of the SiO_2 overcoat. As one crosses the crater, the spectra change significantly due to mixing and loss of material. The spectrum corresponding to a spot inside the edge of the crater shows the loss of the overcoat and 5 or 6 pairs of silica/hafnia layers. It also shows that these are the outer layers of the coating. The next spot in the direction toward the bottom of the crater shows additional loss of hafnia and silica. The layered structure is absent indicating interlayer mixing. The last two spectra show successively greater loss of coating material toward the center of the pit.

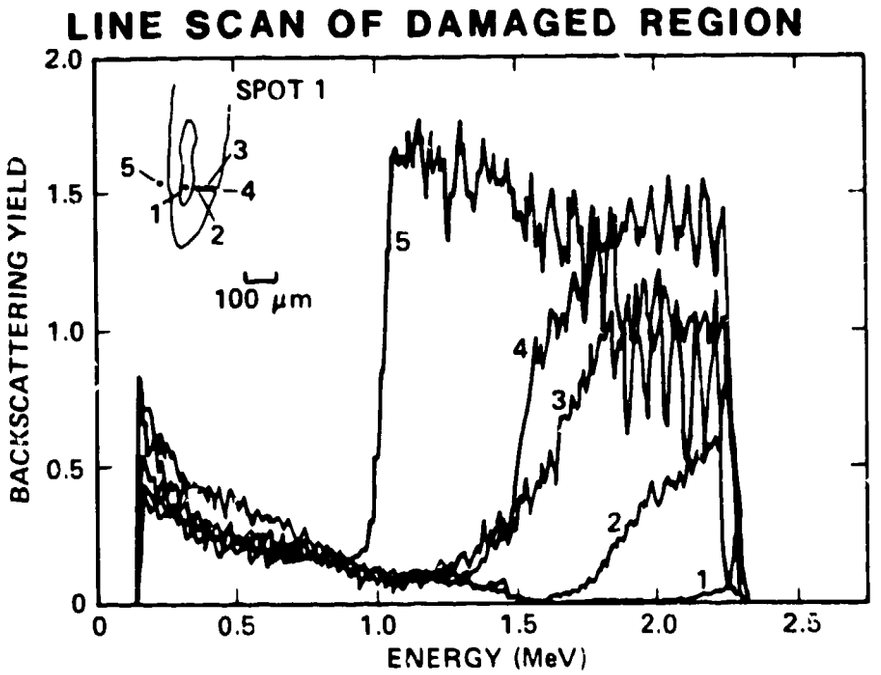

Figure 5. Composite of five RBS energy spectra taken near and on damaged spot. Reflector is SiO_2/HfO_2.

The RBS technique is sensitive to thin overlayers such as the half-wave overcoat of low-index material commonly applied to these mirrors. For example, figure 6 consists of a spectrum from the undamaged region of the SiO_2/HfO_2 mirror over-layed with a spectrum near the damaged area. The small shift in the energy of the upper edge of the hafnium corresponds to a 160 A loss of the SiO_2 overcoat. In addition, the valleys of the undamaged spectrum are deeper than those of the damaged one. This indicates that sub-surface diffusion occurred near the damaged spot. These results suggest that in these hafnia/silica contings, the damage mechanism proceeds from the top toward the substrate.

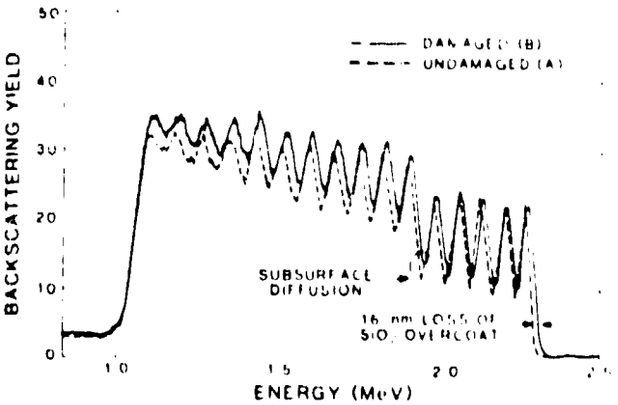

Figure 6. RBS spectra taken from undamaged and slightly damaged regions of SiO_2/HfO_2 showing partial loss of overcoat and diffusion.

Figure 7 shows the RBS spectrum of an undamaged MgF_2/ThF_4 coating using a 100-micron spot size. The 19 layers of thorium fluoride are clearly visible. Note the similarity of this spectrum and that of figure 2. As one approaches the laser-damaged area, the differences between the damage behavior of the SiO_2/HfO_2 and that of the MgF_2/ThF_4 become evident. These differences are shown in figure 8 for line scan data taken using a 10-micron spot size. The spectrum taken near the edge of the damage region exhibits a loss of layered structure near the substrate whereas the thorium peak is enhanced for the top layer. As we move toward the center of the damage region we observe complete loss of structure and 50% reduction in the amount of thorium. In addition, the surface thorium peak gradually disappears. Changes in the slope of the spectra at 0.9 and 1.2 MeV show the presence of flourine and magnesium in the damage area. We believe that this indicates mixing of the magnesium fluoride and thorium fluoride films. The behavior of the surface thorium peak in these data coupled with other spectra from regions which are not visibly altered, indicate that a significant amount of fluorine leaves the surface region. These spectra suggest that the damage mechanism starts from the substrate and progresses outward through the coating.

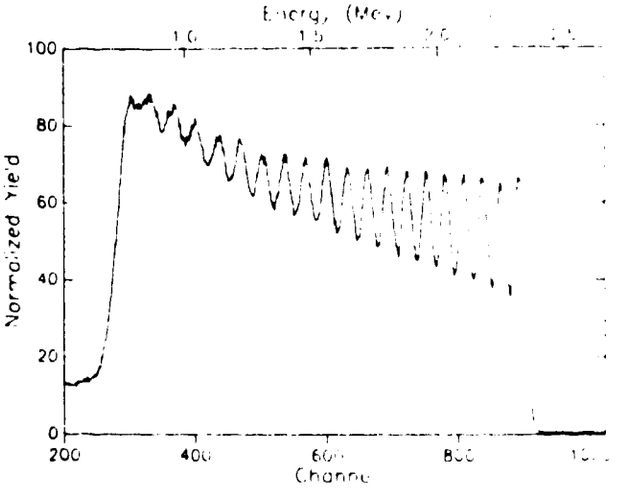

Figure 7. RBS energy spectrum from undamaged region of MgF_2/ThF_4 reflector.

We have also used PIXE to search for low concentration impurities. Figure 9 shows a spectrum obtained by bombarding the SiO_2/HfO_2 sample with a beam of 2.0 MeV protons. In addition to the hafnium L lines, K-α lines from iron and zirconium impurities can be seen. The Fe is present at a concentration of 0.14 and the Zr at 0.29 atomic percent relative to the Hf.

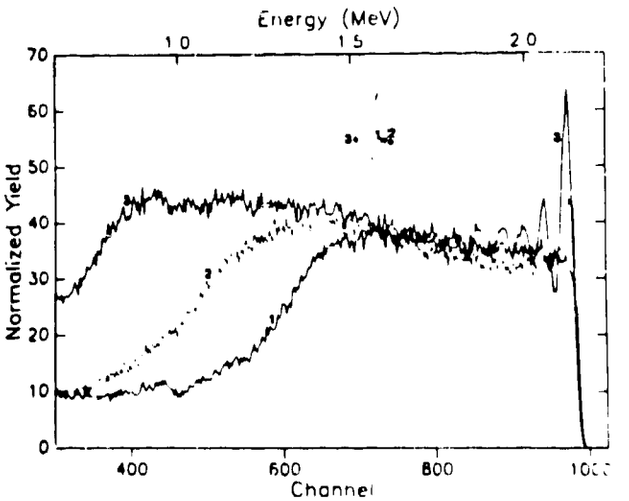

Figure 8. Composite of three energy spectra taken near and on damaged spot. Reflector is MgF_2/ThF_4.

4. Conclusions

Spatially resolved RBS provides detailed information about laser damage mechanisms in multilayer dielectric coatings. Our results show that the fabrication process can result in some interlayer mixing, particularly for those layers closest to the substrate. In addition, the data allow us to identify different damage processes for the two coatings under study. In the case of SiO_2/HfO_2, the interlayer mixing progresses from the surface toward the substrate. For the MgF_2/ThF_4, coating the process is more complex, involving subsurface mixing and loss of near surface fluorine.

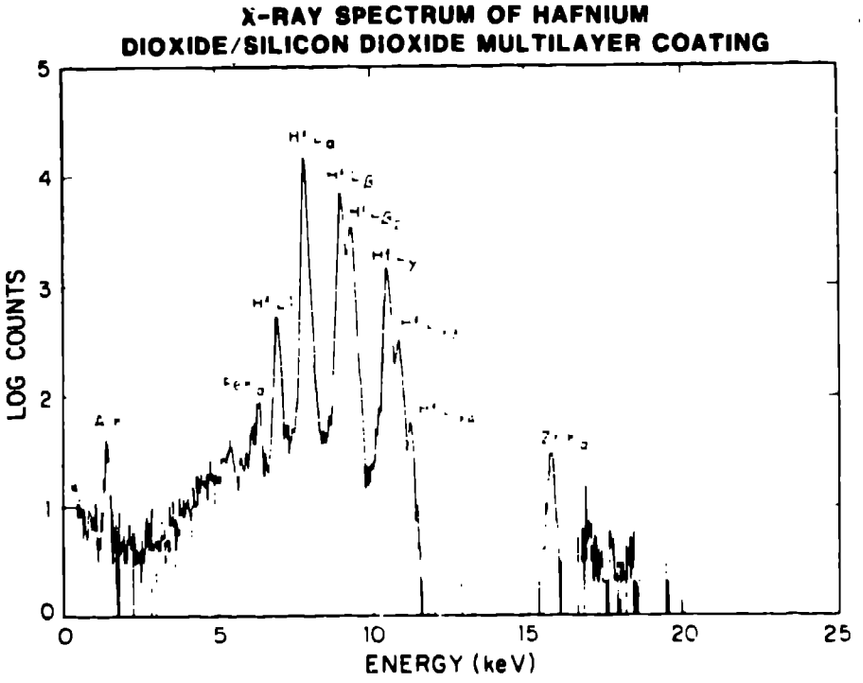

Figure 9. PIXE spectrum from SiO_2/HfO_2 reflector.

We thank Larry Doolittle for providing us with an RBS simulation code and for guidance in operating the code. We are grateful to Lev Borodovsky for helping with the experimental runs and the computer simulations. The experiment would not have been possible without the assistance of Joe Tesmer and the operating staff of the Van de Graaff facility at Los Alamos National Laboratory.

*This work is supported by the Department of Defense.

5. References

[1] W-K. Chu, J. W. Mayer, and M-A. Nicolet, Backscattering Spectrometry, (Academic Press, New York, 1978).

[2] T. B. Johnson, R. Akelsson, and S. A. E. Johansson, Nucl. Instr. Meth. 84, 141 (1970).

[3] J. A. Cookson, "The Production and Use of A Nuclear Microprobe of Ions at MeV Energies," Nuclear Inst. Methods, 65, 477 (1979).

[4] C. Maggiore, "Materials Analysis with a Nuclear Microprobe," Scanning Elect. Microsc., 1, 439 (1980).